HHS Public Access

Author manuscript

Nat Immunol. Author manuscript; available in PMC 2017 September 05.

Published in final edited form as:

Nat Immunol. ; 12(7): 616–623. doi:10.1038/ni.2051.

A semi-invariant $V_\alpha 10^+$ T cell antigen receptor defines a population of natural killer T cells with distinct glycolipid antigen–recognition properties

Adam P Uldrich[1,7], **Onisha Patel**[2,7], **Garth Cameron**[1], **Daniel G Pellicci**[1], **E Bridie Day**[1], **Lucy C Sullivan**[1], **Konstantinos Kyparissoudis**[1], **Lars Kjer-Nielsen**[1], **Julian P Vivian**[2], **Benjamin Cao**[3], **Andrew G Brooks**[1], **Spencer J Williams**[3], **Petr Illarionov**[4], **Gurdyal S Besra**[4], **Stephen J Turner**[1], **Steven A Porcelli**[5], **James McCluskey**[1], **Mark J Smyth**[1,6], **Jamie Rossjohn**[2], and **Dale I Godfrey**[1]

[1]Department of Microbiology and Immunology, The University of Melbourne, Parkville, Victoria, Australia

[2]ARC Centre of Excellence in Structural and Functional Microbial Genomics, Department of Biochemistry and Molecular Biology, Monash University, Clayton, Victoria, Australia

[3]School of Chemistry and Bio21 Molecular Science and Biotechnology Institute, The University of Melbourne, Parkville, Victoria, Australia

[4]School of Biosciences, University of Birmingham, Edgbaston, Birmingham, UK

[5]Department of Microbiology and Immunology, Albert Einstein College of Medicine, Bronx, New York, USA

[6]Peter MacCallum Cancer Centre, East Melbourne, Victoria, Australia

Abstract

Type I natural killer T cells (NKT cells) are characterized by an invariant variable region 14–joining region 18 ($V_\alpha 14$-$V_\alpha 18$) T cell antigen receptor (TCR) α-chain and recognition of the glycolipid α-galactosylceramide (α-GalCer) restricted to the antigen-presenting molecule CD1d. Here we describe a population of α-GalCer-reactive NKT cells that expressed a canonical $V_\alpha 10$-$J_\alpha 50$ TCR α-chain, which showed a preference for α-glucosylceramide (α-GlcCer) and bacterial

Correspondence should be addressed to J.R. (jamie.rossjohn@monash.edu) or D.I.G. (godfrey@unimelb.edu.au).

[7]These authors contributed equally to this work.

Accession codes. Protein Data Bank: $V_\alpha 10$ complex, 3RUG; $V_\alpha 10$ TCR not bound to a ligand, 3AXL.

Note: Supplementary information is available on the Nature Immunology website.

AUTHOR CONTRIBUTIONS

A.P.U. identified and carried out cellular and molecular characterization of $V_\alpha 10$ NKT cells and produced protein complexes for crystallographic studies; O.P. solved the crystal structures and did structural analysis; G.C. and K.K. carried out studies of glycolipid specificity and function; L.C.S. did surface plasmon resonance studies; D.G.P., E.B.D., L.K.-N., J.P.V., S.J.T., G.S.B., B.C., A.G.B., S.J.W., P.I., S.A.P., J.M., M.J.S., J.R. and D.I.G. provided intellectual input and key reagents and assisted with experimental design and interpretation and writing of the manuscript; and M.J.S., J.R. and D.I.G. led the investigation together and devised the project and contributed equally to this work.

COMPETING FINANCIAL INTERESTS

The authors declare competing financial interests: details accompany the full-text HTML version of the paper at http://www.nature.com/natureimmunology/.

α-glucuronic acid–containing glycolipid antigens. Structurally, despite very limited TCRα sequence identity, the $V_α10$ TCR–CD1d–α-GlcCer complex had a docking mode similar to that of type I TCR–CD1d–α-GalCer complexes, although differences at the antigen-binding interface accounted for the altered antigen specificity. Our findings provide new insight into the structural basis and evolution of glycolipid antigen recognition and have notable implications for the scope and immunological role of glycolipid-specific T cell responses.

Natural killer T cells (NKT cells) arise in the thymus through random T cell antigen receptor (TCR) gene-recombination events that result in the expression of TCRs that preferentially interact with lipid-based antigens presented by CD1d on cortical thymocytes[1]. This unusual form of positive selection diverts developing thymocytes into the NKT cell lineage, which is characterized by rapid and diverse cytokine production and multipotent immunoregulatory abilities. NKT cells are traditionally categorized into two distinct populations: type I and type II (ref. 1). Type I NKT cells express an invariant α-chain variable region 14–α-chain joining region 18 ($V_α14$-$J_α18$; TRAV11-TRAJ18) TCR α-chain in mice or $V_α24$-$J_α18$ (TRAV10-TRAJ18) in humans and can recognize the prototypical glycolipid antigen α-galactosylceramide (α-GalCer). Type II NKT cells are also CD1d restricted but do not express this invariant TCR α-chain or recognize α-GalCer. Instead, type II NKT cells express a range of TCRs[2], although they seem to be enriched for TCRs that incorporate $V_α3.2$-$J_α9$ and $V_α8$ (ref. 3) and recognize distinct glycolipid antigens such as sulfatide[4]. Mainly because CD1d–α-GalCer tetramers are the tool of choice for the study of NKT cells, most studies of glycolipid-reactive T cells have focused on type I NKT cells. The invariant $V_α14$-$J_α18$ TCR α-chain is a defining feature of type I NKT cells to the extent that these cells are not detected in mice with deletion of the gene encoding $J_α18$ (*Tcra-J*^{m1Tgi} mice; called '*Jα18*$^{-/-}$ mice' here)[5], now commonly used as a model of deficiency in type I NKT cells. Furthermore, differences between *Jα18*$^{-/-}$ mice and mice with deletion of the gene encoding CD1d (*Cd1d*$^{-/-}$ mice) are presumed to indicate a role for type II NKT cells, which are still present in the former strain but not the latter strain[6–9]. Although human $V_α24^-$ NKT cells reactive to the CD1d–α-GalCer tetramer have been described[10–12], these cells retain the $J_α18$ junctional region that characterizes type I NKT cells[10,12].

Type I NKT cells are stimulated by an array of microbial and self-derived lipid-based antigens[13]. Given the invariant nature of the NKT cell TCR α-chain, this suggests that the NKT cell TCR β-chain has a role in determining differences in antigen specificity. Indeed, mouse NKT cells, which have a more diverse $V_β$ repertoire than do humans, frequently use three $V_β$ genes ($V_β8$, $V_β7$ and $V_β2$; TRBV13, TRBV29 and TRBV1, respectively). The structures of various type I NKT cell TCR–CD1d–antigen complexes[14–18] have provided insight into the basis of type I NKT cell recognition and some clues about the role of differences in $V_β$ use. In all NKT cell TCR–CD1d–antigen structures solved so far, a conserved, tilted and parallel docking mode relative to the CD1d antigen-binding cleft has been observed. In this common framework, the invariant NKT cell TCR α-chain, and in particular the $J_α18$ complementarity-determining region 3 (CDR3) α-loop, dominates the interaction with CD1d. Further, NKT cell TCR-mutagenesis experiments have demonstrated the importance of the $V_α14$ and $V_α24$ CDR1α and $J_α18$ CDR3α loops in interacting with CD1d when they are bound to a diverse array of lipid-based antigens[19–22]. Although

differences are observed in the way $V_\beta 8.2$ and $V_\beta 7$ NKT cell TCRs interact with CD1d, the overall docking mode is largely conserved. Collectively, these studies suggest that the invariant $V_\alpha 14$-$J_\alpha 18$ α-chain has the principal role in determining the conserved NKT cell TCR-CD1d docking topology.

Here we define a previously unknown population of $V_\alpha 10$-$J_\alpha 50^+$ NKT cells (called '$V_\alpha 10$ NKT cells' here) that fits neither the type I nor the type II NKT cell category. Analogous to classical type I NKT cells, the $V_\alpha 10$ NKT cells were defined by a previously unknown canonical TCR α-chain rearrangement and shared some functional attributes with type I cells, including CD1d-mediated recognition of α-GalCer, but recognized other glycolipids differently, including self and bacterial lipids. Here we provide an analysis of several key attributes of this NKT cell subset, including TCR use, antigen reactivity, functional responses and the structural basis of antigen recognition by $V_\alpha 10$ NKT cells.

RESULTS

Identification of T cells reactive to CD1d-α–GalCer in $J_\alpha 18^{-/-}$ mice

$J_\alpha 18^{-/-}$ mice are considered to completely lack type I NKT cells reactive to CD1d–α-GalCer[1]; however, we observed a small population of cells reactive to the CD1d–α-GalCer tetramer in the thymus and liver of $J_\alpha 18^{-/-}$ mice that was absent from $Cd1d^{-/-}$ mice (Fig. 1a). This population was most obvious on the BALB/c background, although it was also detectable in C57BL/6 mice, and was most prominent after enrichment by depletion of $CD8^+$ and $CD24^+$ thymocytes. Similar to BALB/c type I NKT cells[23] (Fig. 1a), these cells could often be categorized into two subsets based on the amount of TCR expression; they also included $CD4^+$ and $CD4^-$ subsets, were $CD44^{hi}$ and $CD69^{int}$ (Fig. 1b) and expressed a TCR V_β repertoire enriched for $V_\beta 8$ and $V_\beta 7$ (Fig. 1c). In C57BL/6 mice, these cells expressed the activating NK cell receptor NK1.1, similar to C57BL/6 type I NKT cells (Fig. 1b). Accordingly, these cells, which lacked the invariant $V_\alpha 14$-$J_\alpha 18$ TCRα yet recognized CD1d–α-GalCer, were representative of neither classical type I NKT cells nor type II NKT cells and represent a previously unrecognized population of NKT cells.

$J_\alpha 18^{-/-}$ NKT cells express a $V_\alpha 10$-$J_\alpha 50$ TCR α-chain

We next determined whether NKT cells derived from $J_\alpha 18^{-/-}$ mice expressed the gene encoding $V_\alpha 14$ or, if not, which genes encoding TCR V_α were used by these cells. RT-PCR-based analysis with a panel of primers for each gene encoding TCR V_α showed a strong band corresponding to $V_\alpha 10$ (TRAV13), but little expression of other V_α genes, apart from a faint band corresponding to $V_\alpha 13$ that sequencing confirmed was nonfunctional (Fig. 2a and data not shown). We then used single-cell RT-PCR analysis to determine the frequency of $V_\alpha 10$ NKT cells. As expected, most conventional T cells (negative for the CD1d–α-GalCer tetramer) did not express $V_\alpha 10$; however, most (14 of 16) of the NKT cells from $J_\alpha 18^{-/-}$ mice reactive to the CD1d–α-GalCer tetramer were $V_\alpha 10^+$ (Fig. 2b). Furthermore, sequence analysis of the PCR products showed that all $V_\alpha 10^+$ NKT cells expressed the gene encoding $J_\alpha 50$ (Table 1). Of 33 $V_\alpha 10^+$ sequences from four independent cell sorts, all included $J_\alpha 50$ and one of five similar CDR3α sequences, each with the same length. Moreover, $V_\alpha 10$ has nine subtypes (TRAV13-1 through TRAV13-5, and TRAV13D-1 through TRAV13D-4), and

all sequences were TRAV13-3 or TRAV13D-3 (which differ by a single amino acid in the framework region), which suggested a potential role for both the CDR1α and CDR2α regions of the $V_α10$ NKT cell TCR in antigen recognition. Sequence analysis of the TCR β-chain with $V_β8.1$- and $V_β8.2$-specific primers showed diverse expression of TCR $J_β$ and diverse length and composition of CDR3β (Table 1). Thus, similar to the $V_α14$ sequence of type I NKT cells, the TCR α-chain sequence of $V_α10$ NKT cells was nearly invariant, whereas the TCR β-chain was heavily biased toward $V_β8$ use but was diverse in the CDR3β region.

The $V_α10$-$J_α50$ TCRα facilitates recognition of CD1d–α-GalCer

Alignment of the sequences of $V_α10$-$J_α50$ and $V_α14$-$J_α18$ showed little homology; moreover, none of the residues with a key role in CD1d-antigen recognition in the $V_α14$-$J_α18$ NKT cell TCR[19–21] were conserved in the $V_α10$-$J_α50$ TCR (Table 1). Therefore, we directly determined whether this TCRα facilitated recognition of CD1d–α-GalCer. We transfected human epithelial 293T cells with rearranged $V_α10$-$J_α50$ or $V_α14$-$J_α18$ TCR α-chains, plus $V_β8.1$ TCR β-chain with a sequence derived from $V_α10$ NKT cells (Table 1, sequence 1) or with $V_β8.3$ or $V_β7$ TCR β-chains derived from irrelevant T cell lines (H-$2D^b$ restricted and influenza A specific), and CD3 complex. The $V_α10$-$J_α50^+$ TCR paired with each TCRβ to support surface expression of αβTCR, and when paired with the $V_β8.1^+$ TCRβ, it conferred recognition of CD1d–α-GalCer (Fig. 2c). The reactivity of the $V_α14$-$J_α18$ TCR α-chain to CD1d–α-GalCer was more permissive, with TCR β-chains $V_β8.1$, $V_β8.3$ and $V_β7$ all conferring binding. Thus, we have identified a previously unknown canonical NKT cell TCR α-chain distinct from $V_α14$-$J_α18$ yet still able to confer recognition of CD1d–α-GalCer when paired with a permissive TCR β-chain. The finding that the irrelevant $V_β8.3$ and $V_β7$ TCR β-chains did not support binding of the CD1d-α-GalCer tetramer suggested that CDR3β is also important for the reactivity of the $V_α10$ NKT cell TCR to the CD1d-α-GalCer tetramer.

Glycolipid recognition by $V_α10$ NKT cells

In addition to recognizing α-GalCer, type I NKT cells can recognize a range of glycosphingolipid antigens. Given the very different amino acid sequences of the $V_α10$-$J_α50$ TCR and the $V_α14$-$J_α18$ TCR of type I NKT cells, we labeled thymocyte samples enriched for $V_α10$ and type I NKT cells with the fluorescent dye CFSE and assessed their proliferative responses *in vitro* to a panel of lipid-based CD1d ligands that included bacterial and self lipid antigens (Fig. 3, Supplementary Fig. 1 and data not shown). Although both types of NKT cells proliferated considerably in response to α-GalCer with a saturated 26-carbon ($C_{26:0}$) acyl chain (KRN7000) and a α-GalCer analog with a di-unsaturated 20-carbon ($C_{20:2}$) acyl chain[24], the strongest proliferative response of $V_α10$ NKT cells was in response to $C_{20:2}$ α-glucosylceramide (α-GlcCer)[25]. The mammalian glycolipids iGb3 and β-GalCer stimulated both types of NKT cells, although the response of $V_α10$ NKT cells to β-GalCer was more variable among experiments (Fig. 3a and data not shown).

To determine if $V_α10$ NKT cells recognize glucose-containing microbial glycolipid ligands, we assessed the proliferation and cytokine production (interferon-γ, interleukin 4 (IL-4), IL-13 and IL-17A) in additional experiments involving coculture of purified CFSE-labeled

$V_\alpha 10$ and type I NKT cells in the presence of purified $CD11c^+$ dendritic cells plus the following antigens: α-glucuronosyl diacylglycerol (α-GlcA-DAG) derived from *Mycobacterium smegmatis* (a mixture of three variants ($C_{19:0}$-$C_{16:0}$, $C_{18:0}$-$C_{16:0}$ and $C_{16:0}$-$C_{19:0}$) at a ratio of 1:1:1 (wt/wt/wt), with one being the naturally occurring glycolipid; Supplementary Fig. 1), α-glucuronosyl ceramide (GSL-1) derived from *Sphingomonas* species, α-GalCer, α-GlcCer and iGb3 (Fig. 3b). Although most $V_\alpha 10$ and type I NKT cells proliferated in response to α-GalCer and α-GlcCer, α-GlcA-DAG elicited a stronger proliferative response from $V_\alpha 10$ NKT cells than from type I NKT cells. Furthermore, $V_\alpha 10$ NKT cells produced 10- to 100-fold more IL-4, IL-13 and IL-17A than did type I NKT cells in response to α-GlcA–DAG. Compared with the response of the control cells without glycolipid, the response of type I NKT cells to this antigen ranged from weak to undetectable. The proliferative response to GSL-1 was similar for $V_\alpha 10$ and type I NKT cells, although we also observed more production of IL-4 and IL-13 by $V_\alpha 10$ NKT cells in response to this glycolipid (albeit to a lesser extent than in response to α-GlcA–DAG). We also detected low concentrations of interferon-γ (<50 pg/ml) in cultures of $V_\alpha 10$ NKT cells in response to these microbial glycolipids. Conversely, type I NKT cells seemed to produce stronger responses to α-GalCer and iGb3.

To determine which of the three α-GlcA-DAG variants stimulated the $V_\alpha 10$ NKT cells, we tested each ligand separately (Fig. 3c). The naturally occurring compound $C_{19:0}$-$C_{16:0}$ α-GlcA-DAG[26] elicited the strongest proliferative response. Dose-response experiments with $C_{19:0}$-$C_{16:0}$ α-GlcA-DAG showed greater stimulation of $V_\alpha 10$ NKT cells at a range of doses from 10 μg/ml down to 0.6 μg/ml (Fig. 3d). Type I NKT cells showed little response at any dose but responded well to the positive control (α-GlcCer; data not shown). These data suggest that although there is some overlap in specificity, $V_\alpha 10$ NKT cells are functionally distinct from type I NKT cells and tend to recognize glucose- and glucuronic acid–containing glycolipids.

Binding affinity of the $V_\alpha 10$ NKT cell TCR

We used a soluble $V_\alpha 10$-$J_\alpha 50$ NKT cell TCR composed of paired TCR α- and β-chains (Table 1, sequence 1) from a $V_\alpha 10$ NKT cell clone carrying a TCR α-chain sequence present in both thymus and liver and measured affinity by surface plasmon resonance (Fig. 4a). As expected, control type I TCRs ($V_\alpha 14$-$J_\alpha 18$–$V_\beta 8.2$ and $V_\alpha 14$-$J_\alpha 18$–$V_\beta 7$; derived from published work[14]) bound to CD1d–α-GalCer with very high affinity (dissociation constants of 41 nM and 170 nM, respectively) and to CD1d–α-GlcCer with approximately 10% as much affinity (dissociation constants of 530 nM and 1.9 μM, respectively). Consistent with the results of the proliferation experiments (Fig. 3a), the $V_\alpha 10$ NKT cell TCR bound to CD1d–α-GlcCer with approximately fivefold higher affinity than it showed for CD1d–α-GalCer (dissociation constants of 4.4 μM and 23 μM, respectively). Thus, $V_\alpha 10$ NKT cell TCRs seemed to preferentially recognize CD1d–α-GlcCer better than CD1d–α-GalCer.

On the basis of those differences in recognition, we determined whether costaining with CD1d tetramers loaded with either α-GlcCer or α-GalCer would allow us to distinguish $V_\alpha 10$ NKT cells from type I NKT cells in wild-type mice. Costaining of thymocytes showed

a minor population that stained more brightly with the α-GlcCer tetramer (Fig. 4b), and a major population was stained more brightly with the α-GalCer tetramer. We assessed the TCR expression of these populations by single-cell PCR. All nine cells with high expression of the CD1d–α-GlcCer tetramer were $V_α10^+$ (Fig. 4b), whereas none were $V_α14^+$ and we successfully sequenced eight of nine as $V_α10\text{-}J_α50^+$ (data not shown). In contrast, only one of nine cells with high expression of the CD1d–α-GalCer tetramer was $V_α10^+$, and sequencing determined that this was a nonproductive $J_α50^-$ rearrangement (data not shown), whereas six of nine of these cells were $V_α14^+$. Thus, $V_α10^+$ NKT cells were present in wild-type mice and could be distinguished from type I NKT cells by costaining with CD1d tetramer loaded with either α-GalCer or α-GlcCer.

The $V_α10$ TCR–CD1d–α-GlcCer ternary complex

We determined the structure of the $V_α10$ TCR–CD1d–α-GlcCer complex at a resolution of 2.2Å (Fig. 5 and Supplementary Table 1). The $V_α10$ TCR adopted a parallel docking mode above the F′ pocket of the CD1d antigen-binding cleft (Fig. 5a,b) in a manner very similar to that of other type I NKT cell TCR–CD1d–α-GalCer complexes (Fig. 5c). However, there was a 14° difference in the docking angles, with the $V_α10$ TCR leaning more toward the F′ pocket than did the type I NKT cell TCR–CD1d–α-GalCer complex (Fig. 5d).

The interactions of the $V_α10$ TCR with CD1d spanned residues 72–87 and 145–154 of the α1 helix and α2 helix, respectively (Supplementary Table 2), which buried ~910$Å^2$ after ligation; this was slightly greater than the buried surface area at the interface of type I NKT cell TCR–CD1d–α-GalCer (buried surface area, 760–860$Å^2$ for $V_β8.2$ and $V_β7$ NKT cell TCRs[14]; Fig. 5b,e). At this interface, the TCR α- and β-chains contributed 59% and 41% of the buried surface area, respectively, with all CDRs contacting CD1d. CDR1α, CDR2α and CDR3α contributed 14%, 13% and 32%, respectively, whereas the CDR1β, CDR2β and CDR3β loops contributed 8%, 21% and 12%, respectively. Thus, whereas the CDR3α and CDR2β loops dominated interactions at the $V_α10$ TCR–CD1d–α-GlcCer interface, the involvement of CDR2α was unique to $V_α10$ NKT cells, in contrast to the type I NKT $V_β8^+$ TCR, in which only CDR1α, CDR3α and CDR2β mediated contact with CD1d–α-GalCer. Thus, the $V_α10$ and $V_α14$ NKT cell TCR–CD1d–antigen complexes showed similar docking modes, despite substantial differences in their $V_α$ and $J_α$ sequences.

$V_α10$ TCR–CD1d interactions

As $V_α10$ shares only 40% sequence identity with $V_α14$, we observed many differences in the interactions mediated by the respective TCR α-chains. In the $V_α10$ complex, Thr28α and Asn30α of CDR1α made van der Waals interactions with Val72 and Asp153 of CD1d, respectively (Fig. 6a), whereas in the type I complex, the CDR1α loop exclusively contacted α-GalCer[14]. The CDR2α loop of $V_α10$ TCR contained a bulky Trp59α residue that made extensive van der Waals interactions with residues spanning Ala152–Gly155 of the α2 helix of CD1d (Fig. 6a and Supplementary Table 2), whereas the corresponding loop in the type I TCR does not mediate any contacts with CD1d–α-GalCer[14] or CD1d–α-GlcCer[17]. $J_α50$-encoded CDR3α interacted with residues from both the α1 and α2 helices of CD1d, including one hydrogen bond (between Ser109α and Asp80). Most notably, the bulky side chain of Phe113α protruded into the binding cleft between the α1 helix and α2 helix and

made van der Waals interactions with Asp80 and Glu83 of the α1 helix and Pro146 and Val149 of the α2 helix (Fig. 6b, Supplementary Table 2). Accordingly, the CDR3α-CD1d interactions in the $V_α10$ complex were dominated by van der Waals contacts, whereas the type I NKT cell TCR CDR3α-CD1d interface was characterized by a large network of polar interactions[14] (Fig. 6c).

$V_β8.1$ shares 87% and 52% sequence identity with $V_β8.2$ and $V_β7$, respectively, and thus many contacts were conserved between the TCR β-chain of $V_α10$ and type I complexes. As noted before for type I NKT cell TCRs[14], the TCR β-chain of the $V_α10$ NKT cell TCR contacted only CD1d (Supplementary Table 2). The interactions between $V_α10$ NKT cell TCR CDR1β and CD1d were mediated by Asp30β and Tyr31β, with Asp30β forming a salt bridge with Lys148, whereas the aromatic side chain of Tyr31β interacted with Val149 (Fig. 6d). These CDR1β-CD1d interactions were absent from the $V_β8.2$ NKT cell TCR–CD1d–α-GalCer complex, whereas the $V_β7$ complex included an equivalent salt bridge (Glu30β-Lys148)[14].

In the CDR2β loop, Tyr55β, Tyr57β and Glu63β contacted CD1d, with Tyr55β and Tyr57β forming hydrogen bonds and van der Waals contacts with Glu83 and Lys86, which also formed a salt bridge with Glu63β. In addition, Tyr57β formed van der Waals interactions with Met87 and Leu145 of the CD1d α1 helix and α2 helix, respectively (Fig. 6e). These interactions were analogous to those mediated by the CDR2β loop of the $V_β8.2$ type I NKT cell TCR[14].

The hypervariable CDR3β loop ‘sat’ above the α2 helix, which allowed Leu108β, Gly109β, Gly113β and Tyr114β to make van der Waals interactions with CD1d (Fig. 6d). This suggests that the CDR3β loop has an important role in the $V_α10$ TCR–CD1d interaction and is consistent with the observation that $V_β8.3$ and $V_β7$ β-chains containing irrelevant CDR3β sequences failed to confer reactivity to the CD1d–α-GalCer tetramer when paired with $V_α10$ (Fig. 2c). Accordingly, despite the similar footprints of the $V_α10$ and type I NKT cell TCRs with CD1d, specific differences at the binding interface were readily apparent.

Plasticity of the $V_α10$ TCR interaction

We also determined the structure of the $V_α10$ NKT cell TCR not bound to a ligand at a resolution of 2.9Å (Supplementary Table 1) and assessed the conformational changes that took place after ligation. In addition to small differences between the TCR alone and in complex in the $V_α$-$V_β$ domain positioning, some of the CDR loops had also moved to allow optimal binding to CD1d–α-GlcCer. In addition to the small change (root mean square deviation (r.m.s.d.), 1.1Å) in the CDR1α loop, we observed notable conformational changes in the CDR3β loop (r.m.s.d., 2.4Å, with maximal shift at Gly109β; data not shown) and CDR3α loop (r.m.s.d., 1.5Å, maximal shift of 2.8Å at Phe113α; Fig. 7a). In the $V_α10$ NKT cell TCR not bound to a ligand, the CDR3β interacted with the tip of CDR3α; however, in the complex, CDR3β moved away from CDR3α, making contacts with the α2 helix of CD1d instead (Fig. 6d). The movement in the CDR3α loop was particularly notable, as reorientation of side-chain residues enabled enhanced contacts with CD1d–α-GlcCer: Ser109α moved toward and formed a hydrogen bond with Asp80 of CD1d, and the Phe113α side chain was orientated to allow contacts with residues from both the α1 helix and α2

helix of CD1d (Fig. 7a). This Phe113α was in a position equivalent to that of Leu99α of the type I TCR (Fig. 6b,c), in which Leu99α was in a small hydrophobic niche formed by Leu84, Leu150 and Val149 of CD1d. Similarly, Phe113α was also in a hydrophobic niche formed by equivalent residues of CD1d. However, the longer side chain of Phe113α protruded further into the CD1d cleft, causing Leu84 and Leu150 to reorientate. The reorientation of Leu84 in turn pushed the tip of the sphingosine tail deeper into the F′ pocket of the binding groove compared with the CD1d-lipid binary complex (Fig. 7a). Thus, in contrast to the rigidity of the type I NKT cell TCR–CD1d–α-GalCer interaction, we observed a greater degree of plasticity for the $V_α10$ NKT cell TCR after interaction with CD1d–α-GlcCer.

Specificity of $V_α10$ TCR for α-GlcCer

The $V_α10$ NKT cell TCR interacted with α-GlcCer solely via the TCR α-chain (Supplementary Table 2), with the sugar directly under the CDR1α loop (Fig. 7b), which allowed the 2′ OH to form a hydrogen bond with Asn30α. In addition, Thr28α and Leu29α of the CDR1α loop made van der Waals interactions with α-GlcCer. Unexpectedly, CDR2α also made contact with the sugar group; Trp59α made van der Waals interactions with the 3′ OH, and there was an H_2O-mediated hydrogen bond between the OH group of Ser58α and the 4′ OH (Fig. 7b). In the CDR3α loop, Ser108α, Ser109α and Ser110α made van der Waals contacts with the glucose as well as the OH groups of the sphingosine tail. Further, the OH group of Ser110α made an H_2O-mediated hydrogen bond with 4′ OH of the sphingosine tail (Fig. 7b). These interactions, characterized by many van der Waals interactions and H_2O-mediated hydrogen bonds were in contrast to the type I NKT cell TCR–α-GalCer interactions, in which many polar OH groups of the galactosyl ring were sequestered by hydrogen bonds with residues from the CDR1α and CDR3α loops (Fig. 7c).

The main difference in the glycosyl head groups of α-GlcCer and α-GalCer was in the orientation of the 4′ OH group. The ‘downward-pointing’ glucosyl 4′ OH group contacted the main chains of Gly155 and Thr156 of CD1d, with Gly155 and its neighboring residues interacting with the CDR2α loop. Accordingly, replacement of α-GlcCer with α-GalCer (Fig. 7b) may have resulted in a destabilizing loss of interactions with CD1d. Moreover, an upward-pointing galactosyl 4′ OH group may have sterically clashed with Ser58α of the CDR2α loop of $V_α10$, a residue that formed an H_2O-mediated hydrogen bond with the glucosyl 4′ OH. Together these data provide a molecular basis for the differences between the type I NKT cell TCR and $V_α10$ NKT cell TCR in their fine specificity for glycolipid antigens.

DISCUSSION

In this study we have identified a unique population of NKT cells that fit neither the type I category nor the type II category; we have called these ‘$V_α10$ NKT cells’. These cells recognized α-GalCer presented by CD1d and were characterized by use of a semi-invariant α-chain ($V_α10$-$J_α50$) and a bias toward $V_β8$ expression. Although the development of $V_α10$ NKT cells remains to be investigated, the very limited junctional diversity and the absence of these cells in *Cd1d*$^{-/-}$ mice suggest that they arise through TCR-mediated intrathymic

selection events in a manner akin to that of type I NKT cells. In further support of that idea, we found that both $CD4^+$ and $CD4^-$ subsets of $V_\alpha10$ NKT cells existed; they were $CD44^{hi}$, $CD69^{lo-int}$ and $NK1.1^+$, they produced large amounts of a range of cytokines, and they were present at greater frequency in liver than spleen (data not shown), which suggests a developmental pathway that makes them more like type I NKT cells than conventional T cells.

The $V_\alpha10$ NKT cells had a hierarchy of antigen reactivity different from that of type I NKT cells[27], as demonstrated by their preferential recognition of α-GlcCer and other glucose-based glyco-lipids, including the microbial glucuronic acid–containing ligand α-GlcA-DAG from *M. smegmatis*[26] and, to a lesser extent, GSL-1 from *Sphingomonas* species[28–30]. The finding that $V_\alpha10$ NKT cells produced 10–100 times more interferon-γ, IL-4, IL-13 and IL-17 in response to α-GlcA-DAG than did type I NKT cells suggested that these cells are functionally distinct. Furthermore, the type of antigen may determine which population dominates the response and may also influence, through differences in cytokine production, the outcome of the response. Further studies are warranted comparing the response of $V_\alpha10$ NKT cells with that of type I NKT cells in mouse-infection studies, especially with bacteria containing glucose-based α-linked glycolipids[26,28–30]. Notably, human $V_\alpha24^-J_\alpha18^+$ type I NKT cells respond less well to α-GlcCer than to α-GalCer[12], which further discriminates between the $V_\alpha10$ NKT cells defined here and human $V_\alpha24^-J_\alpha18^+$ NKT cells. Although CD1d-mediated intrathymic selection seems to impose limitations on TCR α-chain diversity, variations in αβTCR use nonetheless imbue CD1d-restricted T cells with a range of antigen specificities and cytokine-producing potential. The finding that these cells recognized and responded to the mammalian glycolipid antigen iGb3 also suggests that they have the potential for self-reactivity in a manner similar to that of iGb3-reactive type I NKT cells[29,31,32].

Although type I and $V_\alpha10$ NKT cells expressed highly disparate TCR α-chains, they docked onto CD1d-glycolipid antigen in a very similar manner. Nevertheless, we observed key differences in the type I and $V_\alpha10$ NKT cell TCR-CD1d-antigen interfaces, which included the CDR2α loop of the $V_\alpha10$ NKT cell TCR in contact with the lipid antigen. Moreover, we observed differences between the type I and $V_\alpha10$ NKT cell TCRs in the degree of structural plasticity after they engaged their respective CD1d-antigen complex. Furthermore, the CDR3α loop of the $V_\alpha10$ NKT cell TCR interacted with CD1d-antigen mainly through van der Waals interactions, in contrast to the polar bond–mediated network of the CDR3α-mediated interactions of the type I NKT cell TCR[14,15]. Collectively, the differences at the antigen-binding interface explain the differences between type I and $V_\alpha10$ NKT cell TCRs in their antigenic specificity. The CDR3α loop is crucial for docking of type I NKT cell TCR–CD1d–antigen[14,15,19–21,33]. However, the $V_\alpha10$ NKT cell TCR docked in a similar manner, which suggests that it may be the NKT cell TCR β-chain that dictates such a conserved NKT cell TCR-CD1d docking topology. In particular, the CDR2β loop of mouse $V_\beta8^+$ and human $V_\beta11^+$ NKT cell TCRs has two tyrosine residues that form a conserved set of interactions with a defined region on CD1d. These observations have resonance with the $V_\beta8.2$-mediated interaction ‘codons’ observed in the major histocompatibility complex–restricted response, in which two conserved tyrosine residues are considered to dictate TCR–major histocompatibility complex bias[34,35]. However, the $V_\beta7$ NKT cell TCR has only one

tyrosine residue in the corresponding CDR2β loop yet docks onto CD1d in a conserved manner[14]. Similarly, mutagenesis studies of the $V_\beta 2$ NKT cell TCR, which has no tyrosine residues in the CDR2β loop, is also predicted to dock onto CD1d in a conserved manner[21]. Thus, the conserved docking topology may be a consequence of the fact that an innate-like TCR must recognize a relatively monomorphic antigen-presenting molecule.

In summary, we have identified a previously unknown population of CD1d-restricted NKT cells with a unique canonical $V_\alpha 10$-$J_\alpha 50$ TCRα chain that recognize a partially but not completely overlapping array of glycolipids, including self and bacterial antigens. Our findings have also identified a feature of the interaction of TCRs with antigen-presenting molecules: although the diverse repertoire of αβTCRs allows them to bind peptide–major histocompatibility complex molecules in a range of docking modes[36], the diversity of the NKT cell TCR repertoire is associated with a conserved CD1d docking mode. Accordingly, our findings highlight a fundamental difference between peptide- and lipid-mediated recognition by the TCR.

ONLINE METHODS

Mice

C57BL/6 and BALB/c mice were derived from the Peter MacCallum Cancer Centre or were from the Walter and Eliza Hall Institute of Medical Research. The following mice were bred at Peter MacCallum Cancer Centre: BALB/c CD1d1.CD1d2-deficient mice (BALB/c *Cd1d*$^{-/-}$; 11 backcrosses; from Jackson Laboratories)[37]; BALB/c $J_\alpha 18$-deficient mice (BALB/c *J*$_\alpha$*18*$^{-/-}$; 10 backcrosses; originally provided by M. Taniguchi)[5]; C57BL/6 Jα18-deficient mice (C57BL/6 *J*$_\alpha$*18*$^{-/-}$; 12 backcrosses; originally provided by M. Taniguchi)[5]; C57BL/6 CD1d-deficient mice (C57BL/6 *Cd1d*$^{-/-}$; 11 backcrosses; originally provided by Jackson Laboratories)[38]. Mice over 6 weeks of age were used in all experiments, which were done in accordance with the Animal Ethics and Experimentation Committee of Peter MacCallum Cancer Centre.

Flow cytometry

Single-cell suspensions of thymus, spleen and liver were made as described[39]. Where indicated, thymocyte samples were enriched for NKT cells by depletion of $CD8^+$ and $CD24^+$ thymocytes as described[39]. Monoclonal antibody to CD16-CD32 (FcR block; 2.4G2; grown in-house) was included in cell-labeling experiments. Cells were stained with the following antibodies (all from BD Pharmingen): antibody to CD3 (anti-CD3; 145-2C11) anti-CD4 (RM4-5), anti-CD8 (53-6.7), anti-CD44 (IM7), anti-CD49b (HMα2), anti-CD69 (H1.2F3), anti-NK1.1 (PK136), anti-TCRβ (H57-597), anti-$V_\beta 2$ (B20.6), anti-$V_\beta 7$ (TR310), anti-$V_\beta 8.1$-$V_\beta 8.2$ (MR5-2), anti-$V_\beta 8.3$ (1B3.3) or rat IgG2b isotype-matched control antibody (A95-1). Mouse CD1d tetramers (produced in-house with a baculovirus-based CD1d expression system originally derived from M. Kronenberg) were loaded with α-GalCer (from Alexis Biochemicals or P. Savage ($C_{24:1}$ PBS-44 analog)). In some cases, CD1d tetramer was loaded with α-GlcCer ($C_{20:2}$ DB06-15 analog[24,25]). In some experiments, 7-amino-actinomycin D (Molecular Probes) and/or unloaded mouse CD1d tetramers were used for the exclusion of dead and nonspecifically stained cells. Cells were

analyzed with an LSR II or FACSCanto (BD Biosciences) and data were processed with FlowJo (Tree Star), with bi-exponential scaling.

In vitro stimulation

For *in vitro* proliferation assays, two approaches were used. In one approach (Fig. 3a), thymocyte samples were depleted of $CD8^+$ and $CD24^+$ cells[39] and labeled for 10 min at 37 °C with 2 μM CFSE (carboxyfluorescein diacetate succinimidyl ester; Molecular Probes), then the thymocytes (1.5×10^5) were cultured for 72 h with 3×10^5 BALB/c $J_\alpha 18^{-/-}$ splenocytes that had been pulsed the night before with α-GalCer ($C_{26:0}$ or $C_{20:2}$; 100 ng/ml), α-GlcCer ($C_{20:2}$; 100 ng/ml)[24,25], β-GalCer (C_{12}; 10 μg/ml; Avanti Polar Lipids) or iGb3 ($C_{26:0}$; 10 μg/ml; Alexis Biochemicals). Glycolipid stock solutions were dissolved in either dimethyl sulfoxide or a solution of 0.5% (vol/vol) Tween-20, sucrose (56 mg/ml) and L-histidine (7.5 mg/ml) and were sonicated for ~15 min immediately before use. For the second approach (Fig. 3b–d), purified $\alpha\beta TCR^+$ thymic NKT cells positive for CD1d–α-GalCer tetramer (1×10^3 to 4×10^3 cells) were labeled with 1 μM CFSE and were cultured for 72 h in 50 μl culture medium in the presence of 2×10^4 splenic $CD11c^+$ dendritic cells (from BALB/c $J_\alpha 18^{-/-}$ mice) with or without the following synthetic glycolipids: $C_{26:0}$ α-GalCer (500 ng/ml), α-GlcCer (500 ng/ml), *M. smegmatis* α-GlcA-DAG (0.6–10 μg/ml; either separate or a mixture of three analogs ($C_{18:0}$-$C_{16:0}$, $C_{19:0}$-$C_{16:0}$ and $C_{16:0}$-$C_{19:0}$) at a ratio of 1:1:1 (wt/wt/wt); structures, Supplementary Fig. 1), *Sphingomonas* species GSL-1 ($C_{14:0}$ α-glucuronosyl ceramide[40]; 1 μg/ml; National Institutes of Health Tetramer Core Facility) or iGb3 (10 μg/ml; Alexis Biochemicals). Cells were cultured in RPMI-1640 medium (Invitrogen Life Technologies) supplemented with 10% (vol/vol) FCS (JRH Biosciences), penicillin (100 U/ml), streptomycin (100 μg/ml), Glutamax (2 mM), sodium pyruvate (1 mM) and nonessential amino acids (0.1 mM) and HEPES buffer (15 mM), pH 7.2–7.5 (all from Invitrogen Life Technologies), plus 50 μM 2-mercaptoethanol (Sigma-Aldrich). Culture supernatants were analyzed for cytokines with a Cytometric Bead Array Mouse Flex Set (BD Biosciences).

Synthesis of α-GlcA-DAG ($C_{19:0}$-$C_{16:0}$)

Three glycolipid variants derived from *M. smegmatis*[26] were synthesized: 1-*O*-((*R*)-10-tuberculostearyl)-2-*O*-palmityl-*sn*-glyceryl α-D-glucopyranosiduronic acid ($C_{19:0}$-$C_{16:0}$;) was prepared from 1-*O*-*tert*-butyldiphenylsilyl-2-*O*-*p*-methoxybenzyl-*sn*-glycerol and 2,3,4-tri-*O*-benzyl-6-*O*-acetyl-α-D-glucopyranosyl iodide, followed by C6-oxidation and esterification (B.C. *et al.*, personal communication). Hydrogenolysis of 1-*O*-((*R*)-10-tuberculostearyl)-2-*O*-palmityl-*sn*-glyceryl (benzyl 2,3,4-tri-*O*-benzyl-α-D-glucuronate) gave the title compound $[\alpha]_D^{23}$ +39.2 (*c* 0.25 in dimethyl sulfoxide), δ_H (500 MHz; dimethyl sulfoxide) 0.81 (d, 3H), 0.85 (t, 6H), 1.03–1.23 (m, 51H), 1.50 (m, 4 H), 2.24–2.31 (m, 4 H), 3.22 (dd, 1H), 3.55 (dd, 1H), 3.69 (dd, 1H), 3.77 (d, 1H), 4.16 (dd, 1H), 4.32 (dd, 1H), 4.69 (d, 1H), 5.11 (m, 1H); δ_C (125 MHz; dimethyl sulfoxide) 13.91, 19.55, 22.09, 24.41, 24.44, 26.40, 26.44, 28.43, 28.45, 28.69, 28.71, 28.76, 28.96, 29.02, 29.07, 29.36, 29.37, 31.29, 32.06, 33.42, 33.53, 36.42, 36.44, 62.19, 65.48, 69.58, 71.38, 71.76, 72.61, 99.37, 171.06, 172.25, 172.53; high-resolution mass spectrometry–electrospray ionization $[M + Na]^+$ calculated for $C_{44}H_{82}O_{11}$, 809.5749; found a mass/charge ratio of 809.5739.

Single-cell PCR and RT-PCR

For analysis of genes encoding V_α regions, RNA was extracted from sorted NKT cells with an RNeasy kit (Qiagen) and cDNA was synthesized with oligo(dT_{15}) primers (Promega) and AMV reverse transcriptase (Promega) in accordance with the manufacturers' instructions. NKT cell cDNA was amplified by PCR with a panel of V_α-specific primers[41] and GoTaq Master Mix (Promega). For single-cell PCR, cDNA from sorted $\alpha\beta TCR^+$ $V_\beta 8^+$ thymic NKT cells positive for CD1d–α-GalCer tetramer was generated[42] and then was amplified by two rounds of semi-nested PCR[43] with sense primers for $V_\alpha 10$ (external, 5′-CCTTGGTTCTGCAGGAGGGGGAG-3′, and internal, 5′-AACGTCGCAGCTCTTTGCAC-3′), $V_\alpha 14$ (external: 5′-TTGTCCGTCAGGGAGAGAACTGC-3′, and internal: 5′-GACACAGGCAAAGGTCTTGTGTCC-3′) or C_α (5′-GAACCTGCTGTGTAC-3′), each used with the C_α antisense primer (both rounds; 5′-TGGCGTTGGTCTCTTTGAAG-3′). PCR products were separated by electrophoresis through a 1.5% agarose gel and were sequenced as described[43]. TCR residue numbering is in accordance with the International ImMunoGeneTics database[44].

Cloning and expression of genes encoding mouse NKT cell TCRs

Paired TCRα and TCRβ sequences from a single $V_\alpha 10$ NKT cell (Table 1, sequence 1 for both TCRα and TCRβ) were used to design a chimeric transcript that also contained a modified human C_α domain to aid in refolding[14]. Sequences codon-optimized for *Escherichia coli* were synthesized (Genscript) and then transferred into a pET30 expression vector (Novagen). Soluble TRAV13D-3-TRAJ50–TRBV13-3-TRBJ2-7 ($V_\alpha 10$-$J_\alpha 50$–$V_\beta 8.1$-$J_\beta 2.7$) and TRAV11-TRAJ18–TRBV13-2 ($V_\alpha 14$-$J_\alpha 18$–$V_\beta 8.2$-$J_\beta 2.1$) NKT cell TCRs were expressed in *E. coli* strain BL21 and inclusion body proteins were prepared, refolded and purified by gel filtration as described[45].

Transfection of 293T cells with TCR

Full-length TCRα transcripts TRAV13D-3 ($V_\alpha 10$; CDR3α sequence 1, Table 1) and TRAV11 ($V_\alpha 14$) were cloned from $V_\alpha 10$ and type I NKT cell cDNA, respectively, by RT-PCR. Full-length TCRβ (TRBV13-3-TRBJ2-7; $V_\beta 8.1$-$J_\beta 2.7$; CDR3β sequence 1, Table 1) was synthesized (Genscript), and TRBV13-1 ($V_\beta 8.3$) and TRBV29 ($V_\beta 7$) were generated from H-$2D^b$-restricted influenza A–specific clones (E.B.D. *et al.*, personal communication). TCR sequences were verified and inserted into the plasmid pMIGII, and 293T cells were transfected with hydrolase element P2A–linked genes encoding CD3, TCRα and TCRβ as described[46]. After 48 h of culture to allow expression of proteins, cells positive for the expression of green fluorescent protein were analyzed for surface expression of TCR by flow cytometry.

Surface plasmon resonance

A ProteOn XPR36 protein-interaction array system (Bio-Rad) was used for surface plasmon resonance as described[14]. Streptavidin was coupled to a GLC Sensor Chip (Bio-Rad) by amine coupling (~500 response units), and biotinylated mouse CD1d–α-GalCer, CD1d–α-GlcCer or unloaded CD1d was captured on a separate flow cell for each (~600 response

units each). Soluble TCRs were serially diluted and simultaneously injected over test and control surfaces at a rate of 30 μl/min. After subtraction of data from the control flow cell (unloaded CD1d), interactions were analyzed with ProteOn Manager software version 2.1 (Bio-Rad) and the Scrubber 2.0a program (Prot version; BioLogic Software), and steady-state dissociation constants were derived at equilibrium.

Crystallization, structure determination and refinement

The V_α10 TCR–CD1d–α-GlcCer ternary complex and the V_α10 TCR not bound to ligand (both at a concentration of 10 mg/ml in 10 mM Tris, pH 8.0, and 150 mM NaCl) were crystallized at 18 °C in 20% (vol/vol) PEG 1500 and 0.1 M 2-(*N*-morpholino)ethanesulfonic acid, pH 6.5, and in 20% (vol/vol) PEG 3350, 0.2 M NaI and 0.1 M bis-Tris-propane, pH 6.5 (Hampton Research), respectively. Crystals were flash-frozen before data collection in crystallization solution containing 25% (vol/vol) glycerol as a cryoprotectant. Data for the ternary complex and the TCR were collected at 100 K on the MX1 beamline and MX2 beamline, respectively, at the Australian Synchrotron (Melbourne). The ternary complex crystals diffracted to 2.2Å and belonged to space group $P2_1$ with two ternary complexes in each asymmetric unit, with an r.m.s.d. of 0.57Å over 784 Cα atoms. Thus, structural analysis was restricted to one complex in the asymmetric unit. The crystals of the TCR not bound to a ligand diffracted to 2.9Å and belong to the space group C2, with two TCR molecules in each asymmetric unit (Supplementary Table 1). Data for the ternary complex were processed with the Mosflm program for integrating single-crystal-diffraction data from area detectors (version 7.0.5)[47] and were scaled with the SCALA scaling and data-merging program from the CCP4 Suite (Collaborative Computational Project, number 4)[48]. The complex was solved by the molecular-replacement method with the MOLREP program in CCP4, with V_α14–Vα8.2 TCR minus the CDR loops (Protein Data Bank accession code, 3HE6) and mouse CD1d minus the lipid (Protein Data Bank accession code, 1Z5L) as the search models. The electron density at the TCR–CD1d–α-GlcCer interface was unambiguous and the initial experimental phases showed an unbiased density for α-GlcCer in the antigen-binding cleft of CD1d. The data for the TCR not bound to a ligand were processed and scaled with the HKL-2000 program package[49]. The structure of the TCR was solved by the molecular-replacement method with the Phaser crystallographic software in CCP4, with V_α14-V_α8.2 NKT cell TCR minus the CDR loops (Protein Data Bank accession code, 3HE6) as a search model. COOT (Crystallographic Object-Oriented Toolkit)[50] was used for model building (Supplementary Table 1). The quality of both structures was confirmed at the Research Collaboratory for Structural Bioinformatics Protein Data Bank Data Validation and Deposition Services website. All presentations of molecular graphics were created with the PyMOL molecular visualization system. For the NKT cell TCR not bound to a ligand, all CDR loops were modeled except CDR2α, which was also involved in crystal contacts and was thus excluded from analysis. For structural analysis, although the structure of the binary complex of CD1d–α-GlcCer was not available, the degree of plasticity in CD1d after engagement of the V_α10 TCR was evaluated by comparison of the V_α10 TCR–CD1d–α-GlcCer in complex with CD1d linked to PBS-25, an analog of α-GalCer with a shorter (C_8) acyl chain[51].

Supplementary Material

Refer to Web version on PubMed Central for supplementary material.

Acknowledgments

We thank M. Taniguchi (Chiba University Graduate School of Medicine) for $J_{\alpha}18^{-/-}$ mice; M. Kronenberg (La Jolla Institute for Allergy and Immunology) for the baculovirus-based CD1d expression system; P. Savage (Brigham Young University) for α-GalCer ($C_{24:1}$ PBS-44 analog); the Australian Synchrotron staff at the MX1 and MX2 beamlines of the Australian synchrotron for assistance with data collection; S. Mattarollo, S. Doak, S. Berzins and A. Denton for discussions and assistance with some experiments; K. Field, N. Sanders and M. Reitsma for assistance with flow cytometry; and M. Stirling and the staff of the Peter MacCallum Cancer Centre Animal House and D. Maksel from the Protein Crystallography Unit at Monash University for technical assistance. Supported by the Cancer Council of Victoria, the National Health and Medical Research Council of Australia (A.P.U., L.C.S., M.J.S. and D.I.G.), the Australian Research Council (D.I.G., O.P. and J.R.), the Cancer Research Institute (G.C.) and the US National Institutes of Health (AI45889 to S.A.P.).

References

1. Godfrey DI, MacDonald HR, Kronenberg M, Smyth MJ, Van Kaer L. NKT cells: what's in a name? Nat. Rev. Immunol. 2004; 4:231–237. [PubMed: 15039760]
2. Cardell S, et al. CD1-restricted $CD4^+$ T cells in major histocompatibility complex class II-deficient mice. J. Exp. Med. 1995; 182:993–1004. [PubMed: 7561702]
3. Park SH, et al. The mouse CD1d-restricted repertoire is dominated by a few autoreactive T cell receptor families. J. Exp. Med. 2001; 193:893–904. [PubMed: 11304550]
4. Blomqvist M, et al. Multiple tissue-specific isoforms of sulfatide activate CD1d-restricted type II NKT cells. Eur. J. Immunol. 2009; 39:1726–1735. [PubMed: 19582739]
5. Cui JQ, et al. Requirement for $V_{\alpha}14$ NKT cells in Il-12-mediated rejection of tumors. Science. 1997; 278:1623–1626. [PubMed: 9374462]
6. Renukaradhya GJ, et al. Type I NKT cells protect (and type II NKT cells suppress) the host's innate antitumor immune response to a B cell lymphoma. Blood. 2008; 111:5637–5645. [PubMed: 18417738]
7. Kim JH, Choi EY, Chung DH. Donor bone marrow type II (non-$V_{\alpha}14J_{\alpha}18$ CD1d-restricted) NKT cells suppress graft-versus-host disease by producing IFN-γ and IL-4. J. Immunol. 2007; 179:6579–6587. [PubMed: 17982047]
8. Terabe M, et al. A nonclassical non- $V_{\alpha}14J_{\alpha}18$ CD1d-restricted (type II) NKT cell is sufficient for down-regulation of tumor immunosurveillance. J. Exp. Med. 2005; 202:1627–1633. [PubMed: 16365146]
9. Berzins SP, Smyth MJ, Godfrey DI. Working with NKT cells—pitfalls and practicalities. Curr. Opin. Immunol. 2005; 17:448–454. [PubMed: 15963710]
10. Gadola SD, et al. Structure and binding kinetics of three different human CD1d-α-galactosylceramide-specific T cell receptors. J. Exp. Med. 2006; 203:699–710. [PubMed: 16520393]
11. Gadola SD, Dulphy N, Salio M, Cerundolo V. V alpha 24-J alpha Q-independent, CD1d-restricted recognition of alpha-galactosylceramide by human $CD4^+$ and $CD8\alpha\beta^+$ T lymphocytes. J. Immunol. 2002; 168:5514–5520. [PubMed: 12023346]
12. Brigl M, et al. Conserved and heterogeneous lipid antigen specificities of CD1d-restricted NKT cell receptors. J. Immunol. 2006; 176:3625–3634. [PubMed: 16517731]
13. Godfrey DI, et al. Antigen recognition by CD1d-restricted NKT T cell receptors. Semin. Immunol. 2010; 22:61–67. [PubMed: 19945889]
14. Pellicci DG, et al. Differential recognition of CD1d-alpha-galactosyl ceramide by the $V_{\beta}8.2$ and $V_{\beta}7$ semi-invariant NKT T cell receptors. Immunity. 2009; 31:47–59. [PubMed: 19592275]
15. Borg NA, et al. CD1d-lipid-antigen recognition by the semi-invariant NKT T-cell receptor. Nature. 2007; 448:44–49. [PubMed: 17581592]

16. Li Y, et al. The $V_{\alpha}14$ invariant natural killer T cell TCR forces microbial glycolipids and CD1d into a conserved binding mode. J. Exp. Med. 2010; 207:2383–2393. [PubMed: 20921281]
17. Wun KS, et al. A molecular basis for the exquisite CD1d-restricted Ag-specificity and functional responses of NKT cells. Immunity. 2011; 34:327–339. [PubMed: 21376639]
18. Mallevaey T, et al. The molecular basis of NKT cell autoreactivity and recognition of self-CD1d. Immunity. 2011; 34:315–326. [PubMed: 21376640]
19. Wun KS, et al. A minimal binding footprint on CD1d-glycolipid is a basis for selection of the unique human NKT TCR. J. Exp. Med. 2008; 205:939–949. [PubMed: 18378792]
20. Scott-Browne JP, et al. Germline-encoded recognition of diverse glycolipids by natural killer T cells. Nat. Immunol. 2007; 8:1105–1113. [PubMed: 17828267]
21. Mallevaey T, et al. T cell receptor CDR2β and CDR3β loops collaborate functionally to shape the iNKT cell repertoire. Immunity. 2009; 31:60–71. [PubMed: 19592274]
22. Florence WC, et al. Adaptability of the semi-invariant natural killer T-cell receptor towards structurally diverse CD1d-restricted ligands. EMBO J. 2009; 28:3579–3590. [PubMed: 19816402]
23. Stenstrom M, Skold M, Andersson A, Cardell SL. Natural killer T-cell populations in C57BL/6 and NK1.1 congenic BALB.NK mice-a novel thymic subset defined in BALB.NK mice. Immunology. 2005; 114:336–345. [PubMed: 15720435]
24. Yu KO, et al. Modulation of CD1d-restricted NKT cell responses by using N-acyl variants of α-galactosylceramides. Proc. Natl. Acad. Sci. USA. 2005; 102:3383–3388. [PubMed: 15722411]
25. Jervis PJ, et al. Synthesis and biological activity of α-glucosyl C24:0 and C20:2 ceramides. Bioorg. Med. Chem. Lett. 2010; 20:3475–3478. [PubMed: 20529677]
26. Wolucka BA, McNeil MR, Kalbe L, Cocito C, Brennan PJ. Isolation and characterization of a novel glucuronosyl diacylglycerol from *Mycobacterium smegmatis*. Biochim. Biophys. Acta. 1993; 1170:131–136. [PubMed: 8399336]
27. Kawano T, et al. Cd1d-restricted and TCR-mediated activation of $V_{\alpha}14$ NKT cells by glycosylceramides. Science. 1997; 278:1626–1629. [PubMed: 9374463]
28. Kinjo Y, et al. Recognition of bacterial glycosphingolipids by natural killer T cells. Nature. 2005; 434:520–525. [PubMed: 15791257]
29. Mattner J, et al. Exogenous and endogenous glycolipid antigens activate NKT cells during microbial infections. Nature. 2005; 434:525–529. [PubMed: 15791258]
30. Sriram V, Du W, Gervay-Hague J, Brutkiewicz RR. Cell wall glycosphingolipids of *Sphingomonas paucimobilis* are CD1d-specific ligands for NKT cells. Eur. J. Immunol. 2005; 35:1692–1701. [PubMed: 15915536]
31. Zhou D, et al. Lysosomal glycosphingolipid recognition by NKT cells. Science. 2004; 306:1786–1789. [PubMed: 15539565]
32. Dias BR, et al. Identification of iGb3 and iGb4 in melanoma B16F10-Nex2 cells and the iNKT cell-mediated antitumor effect of dendritic cells primed with iGb3. Mol. Cancer. 2009; 8:116–129. [PubMed: 19968878]
33. Kjer-Nielsen L, et al. A structural basis for selection and cross-species reactivity of the semi-invariant NKT cell receptor in CD1d/glycolipid recognition. J. Exp. Med. 2006; 203:661–673. [PubMed: 16505140]
34. Feng D, Bond CJ, Ely LK, Maynard J, Garcia KC. Structural evidence for a germline-encoded T cell receptor-major histocompatibility complex interaction 'codon'. Nat. Immunol. 2007; 8:975–983. [PubMed: 17694060]
35. Dai S, et al. Crossreactive T Cells spotlight the germline rules for αβ T cell-receptor interactions with MHC molecules. Immunity. 2008; 28:324–334. [PubMed: 18308592]
36. Godfrey DI, Rossjohn J, McCluskey J. The fidelity, occasional promiscuity, and versatility of T cell receptor recognition. Immunity. 2008; 28:304–314. [PubMed: 18342005]
37. Smiley ST, Kaplan MH, Grusby MJ, Immunoglobulin E. Production in the absence of interleukin-4-secreting Cd1-dependent cells. Science. 1997; 275:977–979. [PubMed: 9020080]
38. Sonoda KH, Exley M, Snapper S, Balk SP, Stein-Streilein J. CD1-reactive natural killer T cells are required for development of systemic tolerance through an immune-privileged site. J. Exp. Med. 1999; 190:1215–1226. [PubMed: 10544194]

39. Crowe NY, et al. Differential antitumor immunity mediated by NKT cell subsets in vivo. J. Exp. Med. 2005; 202:1279–1288. [PubMed: 16275765]
40. Long X, et al. Synthesis and evaluation of stimulatory properties of Sphingomonadaceae glycolipids. Nat. Chem. Biol. 2007; 3:559–564. [PubMed: 17660835]
41. Casanova JL, Romero P, Widmann C, Kourilsky P, Maryanski JL. T cell receptor genes in a series of class I major histocompatibility complex-restricted cytotoxic T lymphocyte clones specific for a *Plasmodium berghei* nonapeptide: implications for T cell allelic exclusion and antigen-specific repertoire. J. Exp. Med. 1991; 174:1371–1383. [PubMed: 1836010]
42. Day EB, et al. The context of epitope presentation can influence functional quality of recalled influenza A virus-specific memory $CD8^+$ T cells. J. Immunol. 2007; 179:2187–2194. [PubMed: 17675478]
43. Kedzierska K, Turner SJ, Doherty PC. Conserved T cell receptor usage in primary and recall responses to an immunodominant influenza virus nucleoprotein epitope. Proc. Natl. Acad. Sci. USA. 2004; 101:4942–4947. [PubMed: 15037737]
44. Lefranc MP, et al. IMGT, the International ImMunoGeneTics database. Nucleic Acids Res. 1998; 26:297–303. [PubMed: 9399859]
45. Garboczi DN, et al. Assembly, specific binding, and crystallization of a human TCR-αβ with an antigenic Tax peptide from human T lymphotropic virus type 1 and the class I MHC molecule HLA-A2. J. Immunol. 1996; 157:5403–5410. [PubMed: 8955188]
46. Holst J, et al. Generation of T-cell receptor retrogenic mice. Nat. Protoc. 2006; 1:406–417. [PubMed: 17406263]
47. Leslie AGW. Joint CCP4 + ESF-EAMCB Newsletter on Protein Crystallography. Recent changes to the MOSFLM package for processing film and image plate data. 1992; 26
48. CCP4 (Collaborative Computational Project, 4). The CCP4 suite: Programs for protein crystallography. Acta Crystallogr. D Biol. Crystallogr. 1994; 50:760–763. [PubMed: 15299374]
49. Otwinoski Z, Minor W. Processing of x-ray diffraction data collected in oscillation mode. Methods Enzymol. 1997; 276:307–326.
50. Emsley P, Cowtan K. Coot: model-building tools for molecular graphics. Acta Crystallogr. D Biol. Crystallogr. 2004; 60:2126–2132. [PubMed: 15572765]
51. Zajonc DM, et al. Structure and function of a potent agonist for the semi-invariant natural killer T cell receptor. Nat. Immunol. 2005; 6:810–818. [PubMed: 16007091]

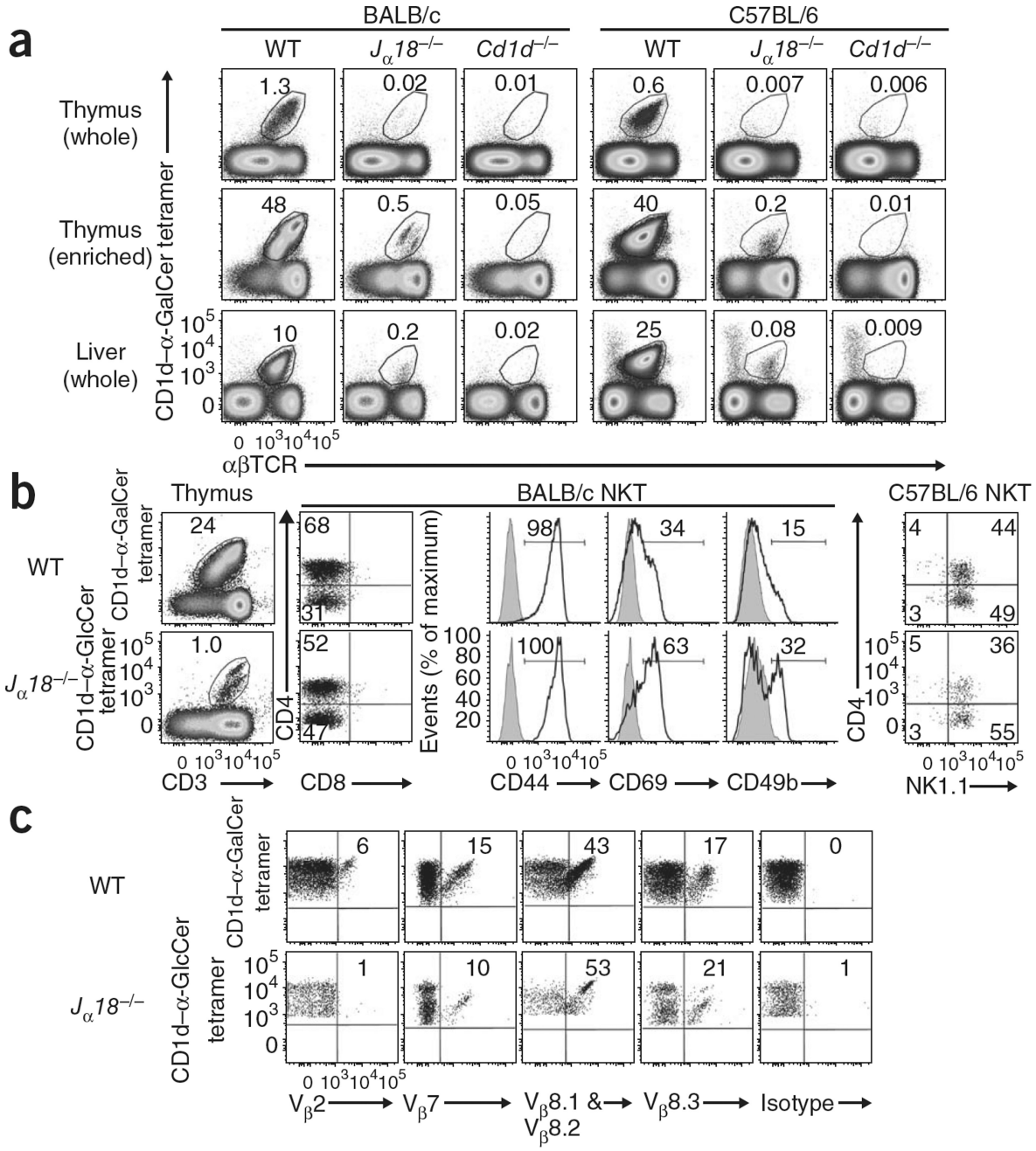

Figure 1.

Identification of $J_\alpha18^{-/-}$ T cells reactive to CD1d–α-GalCer. (**a**) Flow cytometry of thymocytes and liver lymphocytes isolated from BALB/c and C57BL/6 wild-type (WT), $J_\alpha18^{-/-}$ and $Cd1d^{-/-}$ mice (n = 7–9 mice per genotype) and stained with tetramer loaded with CD1d–α-GalCer and monoclonal antibody to αβTCR; thymocyte populations were also enriched for NKT cells by complement-mediated depletion of $CD24^+$ and $CD8^+$ thymocytes. Numbers above outlined areas indicate percent tetramer-positive $\alpha\beta TCR^+$ cells. (**b**) Expression of CD4 versus CD3, CD8, CD44, CD69 and CD49b (black lines) and isotype-matched control antibody staining (gray shading) on NKT cells reactive to CD1d–α-

GalCer (BALB/c wild-type cells) or CD1d–α-GlcCer (BALB/c $J_{\alpha}18^{-/-}$ cells); right, expression of CD4 and NK1.1 in NKT cells from mice on the C57BL/6 background. Numbers above outlined areas, in quadrants or above bracketed lines, indicate percent positive cells in each area. (**c**) Expression of various TCRβ V_{β} regions by NKT cells from BALB/c wild-type and $J_{\alpha}18^{-/-}$ mice. Numbers in quadrants indicate percent positive cells in each. Data are representative of three (**a**) or two (**b**,**c**) separate experiments.

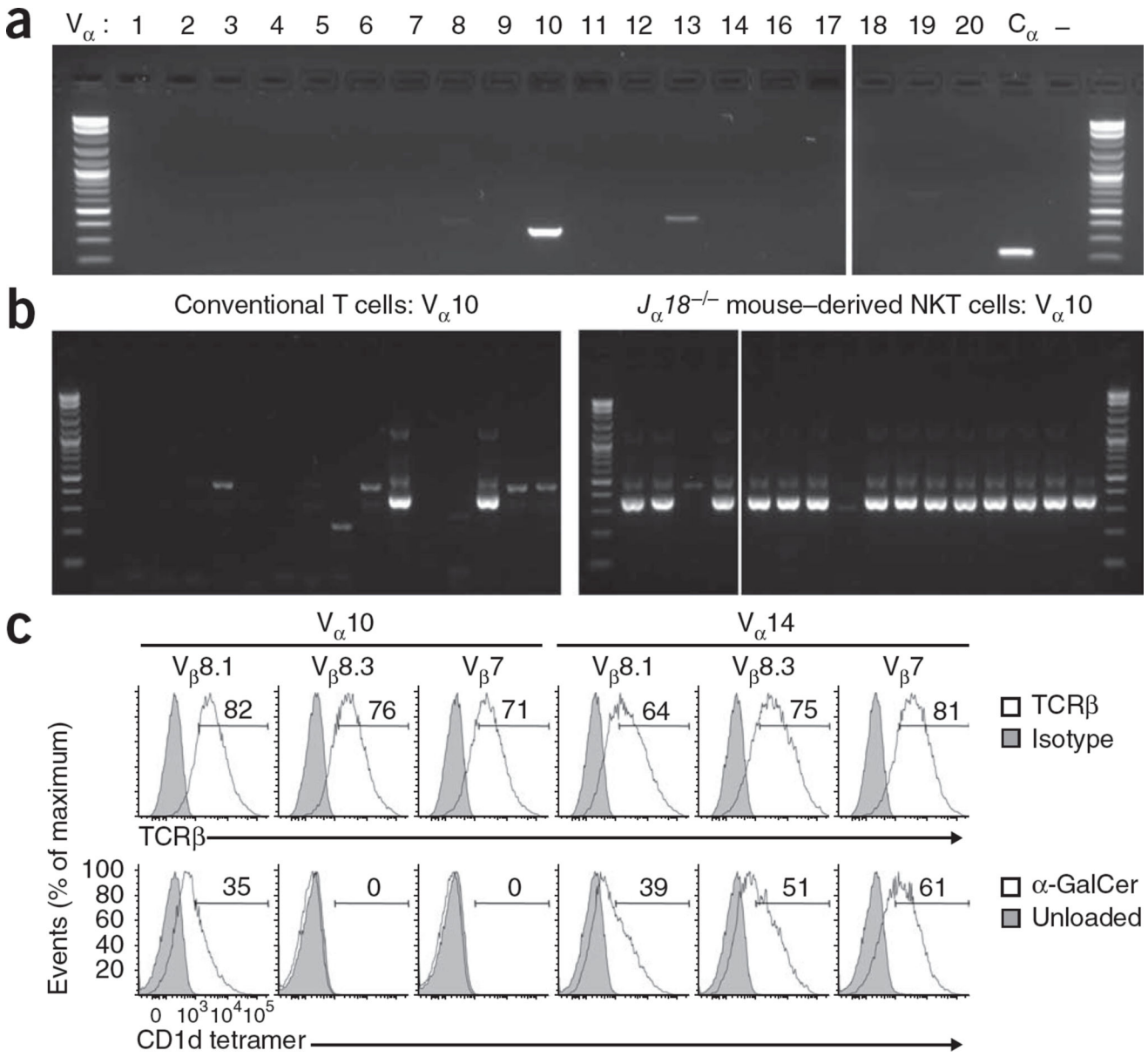

Figure 2.

Jα18$^{-/-}$ CD1d–α-GalCer^{+} NKT cells express a semi-invariant Vα10-Jα50–Vβ8^{+} TCR. (a) PCR analysis of cDNA isolated from CD1d–α-GalCer-reactive cells sorted from BALB/c *Jα18*$^{-/-}$ thymuses and amplified with a panel of primers specific for each TCRα V-gene segment or the α-chain constant region (Cα). – (far right), Cα primers with no cDNA. (**b**) Single-cell PCR analysis for Vα10 on cDNA isolated from Vβ8.1 and Vβ8.2^{+} cells positive for CD1d–α-GalCer tetramer (right; *Jα18*$^{-/-}$ mouse–derived) or Vβ8.1 and Vβ8.2^{+} CD4^{+} αβTCR^{+} cells negative for the CD1d–α-GalCer tetramer (left; conventional T cells) sorted from BALB/c *Jα18*$^{-/-}$ thymuses; $n = 16$ cells per panel. (**c**) Staining of surface TCRβ (top row) and unloaded or α-GalCer-loaded CD1d tetramer (bottom row) on green fluorescent protein–gated human epithelial 293T cells transfected to express full-length rearranged Vα10-Jα50 or Vα14-Jα18 TCR α-chain, plus Vβ8.1, Vβ8.3 or Vβ7 TCR β-chain, and CD3

complex. Isotype, isotype-matched control antibody. Numbers above bracketed lines indicate percent-positive cells. Data are from one experiment (**a**,**b**; one for each) or are representative of one (V_β8.1) or two (V_β8.3 and V_β7) experiments (**c**).

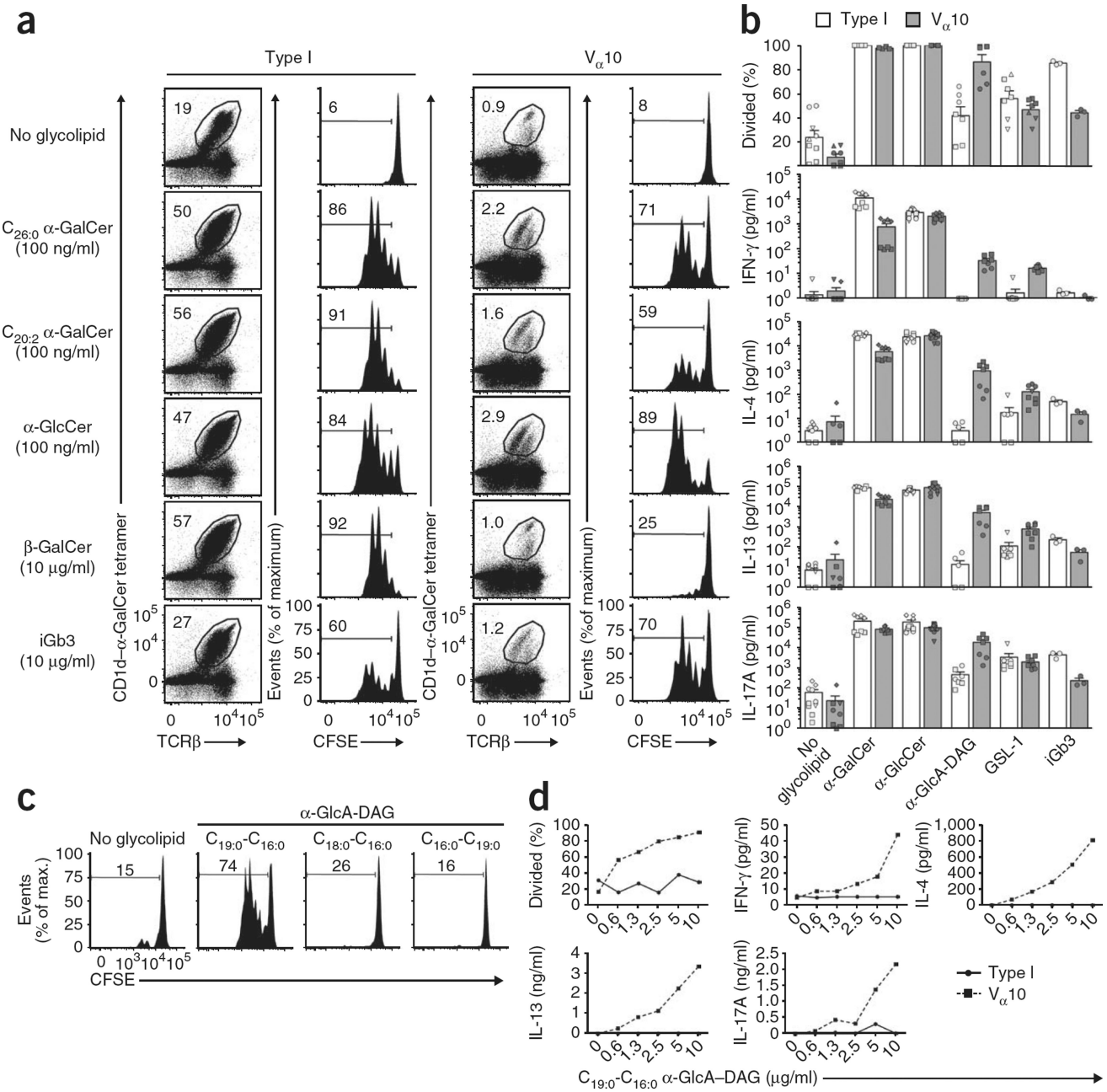

Figure 3.

$V_{\alpha}10$ NKT cells have a unique hierarchy of antigen recognition. (**a**) Frequency of NKT cells among thymocyte populations obtained from BALB/c wild-type and $J_{\alpha}18^{-/-}$ mice, depleted of $CD8^{+}$ and $CD24^{+}$ cells and cultured for 72 h with glycolipid-pulsed antigen-presenting cells ($J_{\alpha}18^{-/-}$ splenocytes), and proliferation of CFSE-labeled type I and $V_{\alpha}10$ NKT cells (gated on CD1d–α-GalCer tetramer, with an additional gate to exclude CFSE spectral overlap (not shown)). Numbers above outlined areas or brackets indicate percent positive cells in each; numbers above bracketed lines indicate percent divided cells. Data are from one of two similar experiments. (**b**) Proliferation (top) and cytokines in supernatants (below) of NKT cells positive for the CD1d–α-GalCer tetramer sorted from BALB/c wild-type and

$J_\alpha 18^{-/-}$ mice, then labeled with CFSE and cultured for 72 h (4×10^3 cells per well) in the presence of no glycolipid, α-GalCer ($C_{26:0}$; 500 ng/ml), α-GlcCer ($C_{20:2}$; 500 ng/ml), α-GlcA–DAG(mixture of variants; 10 μg/ml), GSL-1 (1 μg/ml) or iGb3 (10 μg/ml), plus 20×10^3 sorted splenic $CD11c^+$ dendritic cells. Each symbol shape represents a different experiment. IFN-γ, interferon-γ. Data are from up to four independent experiments (mean and s.e.m. of three to twelve replicates). (**c**) Proliferation of gated $V_\alpha 10$ NKT cells positive for the CD1d–α-GalCer tetramer, sorted from BALB/c $J_\alpha 18^{-/-}$ thymus, labeled with CFSE and cultured for 72 h in the presence (1×10^3 cells per well) or absence (5×10^3 cells per well) of α-GlcA-DAG (10 μg/ml), plus sorted $CD11c^+$ dendritic cells (20×10^3 per well). Numbers above bracketed lines indicate percent divided cells. Data are from one experiment with two replicates. (**d**) Proliferation and cytokine concentrations in supernatants of NKT cells positive for the CD1d–α-GalCer tetramer, sorted from BALB/c wild-type thymus (type I) or $J_\alpha 18^{-/-}$ thymus ($V_\alpha 10$), labeled with CFSE and cultured for 72 h (2×10^3 cells per well) with 20×10^3 sorted $CD11c^+$ dendritic cells and doubling dilutions of $C_{19:0}$-$C_{16:0}$ α-GlcA-DAG. Data are from one of two similar experiments (mean of duplicate cultures).

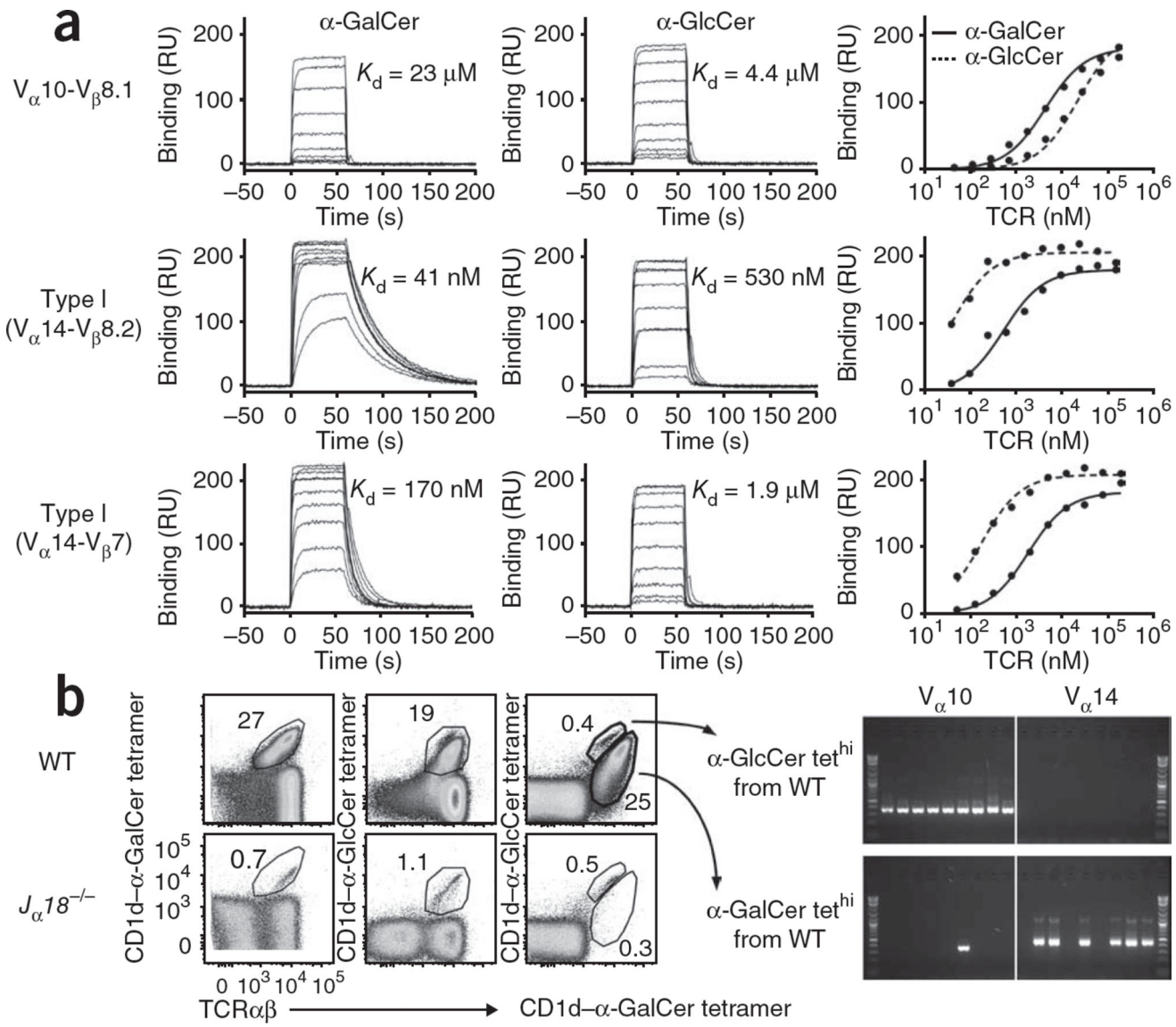

Figure 4.

$V_\alpha 10$ NKT cells have a higher affinity for α-GlcCer and are present in wild-type mice. (**a**) Binding of graded concentrations of $V_\alpha 10$ soluble TCR ($V_\alpha 10$–$V_\beta 8.1$ (175–0.05 μM)) or type I soluble TCR ($V_\alpha 14$–$V_\beta 8.2$ (150–0.04 μM) or $V_\alpha 14$–$V_\beta 7$ (200–0.05 μM)) to CD1d–α-GalCer or CD1d–α-GlcCer, after subtraction of results from those of a control flow cell (unloaded CD1d). Far right, saturation plots showing equilibrium binding to immobilized CD1d–α-GalCer or CD1d–α-GlcCer and the equilibrium dissociation constant (K_d) derived by equilibrium analysis. RU, response units. Data are representative of two independent experiments. (**b**) Staining profiles of α-GalCer tetramer (left) and α-GlcCer tetramer (middle) and dual tetramer labeling (right) in BALB/c wild-type or $J_\alpha 18^{-/-}$ thymocyte populations depleted of $CD8^+$ and $CD24^+$ cells, then simultaneously costained with CD1d tetramers loaded with α-GalCer and α-GlcCer. Numbers adjacent to outlined areas indicate percent cells in each. Far right, single-cell PCR analysis of $V_\alpha 10$ and $V_\alpha 14$ on wild-type

NKT cells with high expression of the α-GlcCer tetramer (α-GlcCer tet^{hi}) or α-GalCer tetramer (α-GalCer tet^{hi}). Data are representative of three independent experiments.

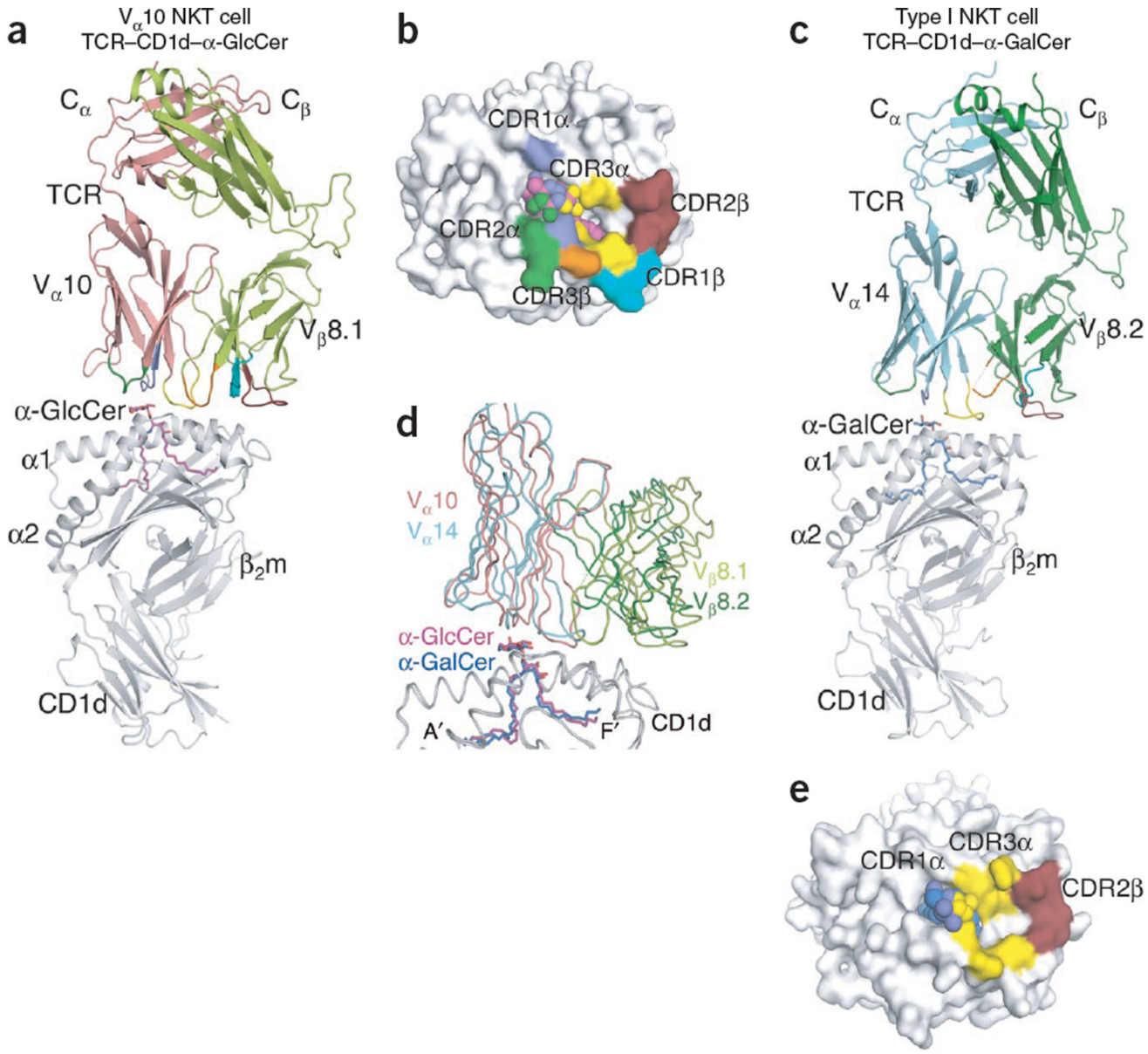

Figure 5.

Structural comparison of $V_\alpha 10$ NKT cell TCR–CD1d–α-GlcCer and type I NKT cell TCR–CD1d–α-GalCer. (**a**) NKT cell $V_\alpha 10$–$V_\beta 8.1$ TCR in complex with CD1d–α-GlcCer: magenta, α-GlcCer; gray, CD1d; salmon, $V_\alpha 10$; light green, $V_\beta 8.1$; purple, CDR1α; dark green, CDR2α; yellow, CDR3α; teal, CDR1β; ruby, CDR2β; orange, CDR3β. β_2m, β_2-microglobulin. (**b**) Footprint of the NKT cell $V_\alpha 10$–$V_\beta 8.1$ TCR on the surface of CD1d–α-GlcCer: spheres indicate α-GlcCer; colors of CD1d and CDR loops as in **a**. (**c**) Type I NKT cell $V_\alpha 14$–$V_\beta 8.2$ TCR in complex with CD1d–α-GalCer[14]: blue, α-GalCer; cyan, $V_\alpha 14$; dark green, $V_\beta 8.2$; colors of CD1d and CDR loops as in **a**. (**d**) Superposition of NKT cell $V_\alpha 10$–$V_\beta 8.1$ TCR–CD1d–α-GlcCer and type I NKT cell $V_\alpha 14$–$V_\beta 8.2$ TCR–CD1d–α-GalCer (colors as in **a**,**c**). (**e**) Footprint of the type I NKT cell $V_\alpha 14$–$V_\beta 8.2$ TCR on the

surface of CD1d–α-GalCer: spheres indicate α-GalCer; colors of CD1d, α-GalCer and CDR loops as in **a**,**c**.

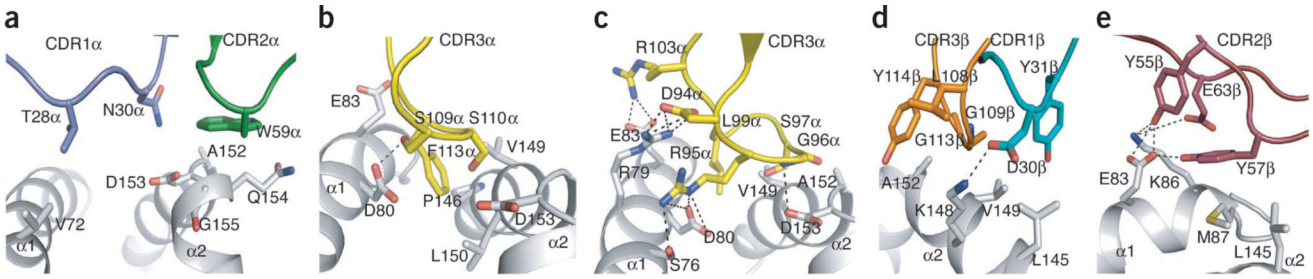

Figure 6.

CD1d-mediated interactions with $V_{\alpha}10$–$V_{\beta}8.1$ NKT cell TCR. (**a**) Contacts of $V_{\alpha}10$ NKT cell TCR CDR1α and CDR2α with CD1d. (**b**) Contacts of $V_{\alpha}10$ NKT cell TCR CDR3α with CD1d. (**c**) Contacts of type I NKT cell TCR CDR3α with CD1d[14]. (**d**) Contacts of $V_{\alpha}10$ NKT cell TCR CDR1β and CDR3β with CD1d. (**e**) Contacts of $V_{\alpha}10$ NKT cell TCR CDR2β with CD1d. Purple, CDR1α; dark green, CDR2α; yellow, CDR3α; teal, CDR1β; ruby, CDR2β; orange, CDR3β; gray, CD1d; black dashed lines, hydrogen bonds and salt-bridge interactions.

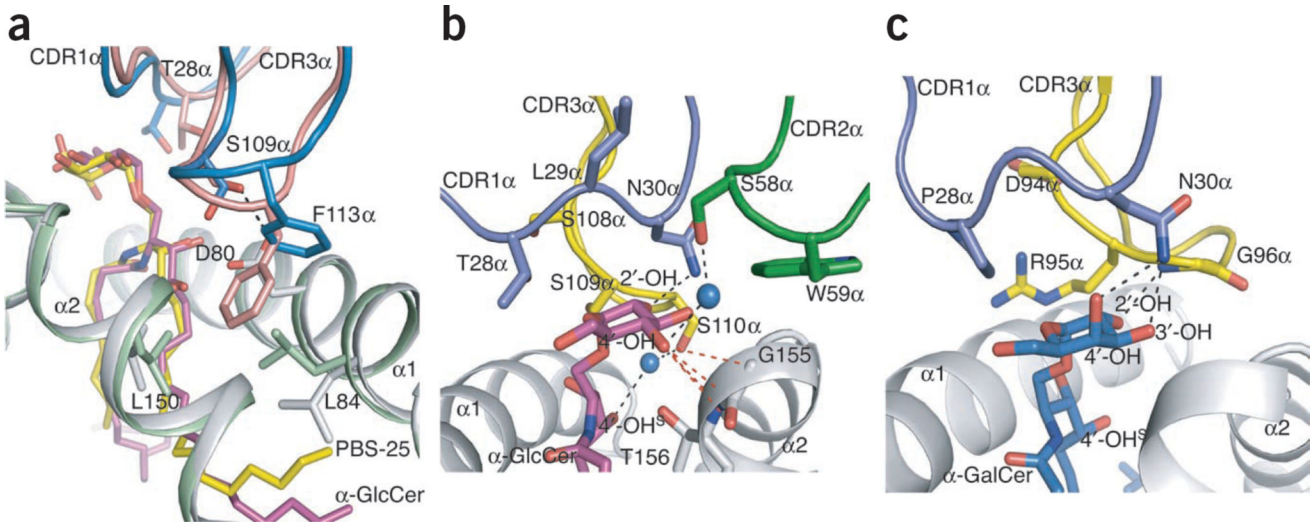

Figure 7.

Lipid antigen specificity. (**a**) Overlay of $V_\alpha 10$ TCR not bound to a ligand and the binary complex of CD1d–PBS-25 (Protein Data Bank accession code, 1Z5L) on the $V_\alpha 10$ TCR–CD1d–α-GlcCer ternary complex: gray, CD1d in the $V_\alpha 10$ complex; magenta, α-GlcCer; salmon, $V_\alpha 10$ TCR in complex; blue, $V_\alpha 10$ TCR not bound to a ligand; light green, CD1d in binary complex; yellow, PBS-25 (α-GalCer analog with a shorter acyl chain). (**b**) Interactions with the $V_\alpha 10$ NKT cell TCR mediated by α-GlcCer: purple, CDR1α; dark green, CDR2α; yellow, CDR3α; magenta, α-GlcCer; gray, CD1d; blue, H_2O molecules; $-OH^S$, −OH on the sphingosine chain. (**c**) Interactions with the type I NKT cell TCR mediated by α-GalCer[14]: blue, α-GalCer; colors of CD1d and CDR loops as in **b**. Black dashed lines, hydrogen bonds; red dashed lines, van der Waals interactions.

Table 1

Sequence analysis of $V_\alpha 10$ NKT cells

TCRα	Gene segment		
Sequence	V_α	V-N	J_α
1	$V_\alpha 10$	^{104}CAIAS	SSFSKLVFGQGTSLSVVP ($J_\alpha 50$)
2	$V_\alpha 10$	^{104}CAIRS	SSFSKLVFGQGTSLSVVP ($J_\alpha 50$)
3	$V_\alpha 10$	^{104}CAMKA	SSFSKLVFGQGTSLSVVP ($J_\alpha 50$)
4	$V_\alpha 10$	^{104}CAMRA	SSFSKLVFGQGTSLSVVP ($J_\alpha 50$)
5	$V_\alpha 10$	^{104}CAMQF	SSFSKLVFGQGTSLSVVP ($J_\alpha 50$)
TCRβ			
Sequence	V_β	V-NDN	J_β
1	$V_\beta 8.1$	^{104}CASRLGG	YEQYFGPGTRLTVL ($J_\beta 2.7$)
2	$V_\beta 8.2$	^{104}CASGDWGA	NTGQLYFGEGSKLTVL ($J_\beta 2.2$)
3	$V_\beta 8.2$	^{104}CASGGTGGR	EQYFGPGTRLTVL ($J_\beta 2.7$)
4	$V_\beta 8.2$	^{104}CASGDWGA	EQYFGPGTRLTVL ($J_\beta 2.7$)
5	$V_\beta 8.1$	^{104}CASRGQG	TEVFFGKGTKLTVV ($J_\beta 1.1$)
6	$V_\beta 8.2$	^{104}CASGAGLGGRD	NYAEQFFGPGTRLTVL ($J_\beta 2.1$)
7	$V_\beta 8.2$	^{104}CASGGRLGG	YAEQFFGPGTRLTVL ($J_\beta 2.1$)
8	$V_\beta 8.2$	^{104}CASSDIWGGH	EQYFGPGTRLTVL ($J_\beta 2.7$)
NKT cell subset	CDR1α	CDR2α	CDR3α
$V_\alpha 10$ ($V_\alpha 10$-$J_\alpha 50$)	TTLNS	SPSWA	CAIASSSFSKLV
Type I ($V_\alpha 14$-$J_\alpha 18$)	VT**P**DN**N**H	LVHEND	CVVG**DRGS**A**LGR**

PCR analysis of unique sequences for TCR α-chains (33 total sequences) and β-chains (13 total sequences) of $V_\alpha 10$ NKT cells sorted from thymus or liver, amplified with primers specific for $V_\alpha 10$, and $V_\beta 8.1$ and $V_\beta 8.2$ (top); and CDR1α, CDR2α and CDR3α sequences from $V_\alpha 10$ and type I NKT cell TCR α-chains (below). Superscripted numbers adjacent to sequences (top) indicate position of first amino acid in sequence; bolding (below) indicates type I NKT cell TCR residues critical for CD1d–α-GalCer interactions. N, nucleotide additions to TCR sequences; D, diversity region.

Data are representative of three (TCRα) or two (TCRβ) separate experiments.